J|A|C|S
ARTICLES
Published on Web 12/08/2001

Structure and Magnetic Properties of Nitroxide Molecular Crystals by Density Functional Calculations Employing Periodic Boundary Conditions

Roberto Improta,[†] Konstantin N. Kudin,[‡] Gustavo E. Scuseria,[‡] and Vincenzo Barone*,[†]

Contribution from the Dipartimento di Chimica, Università Federico II, Complesso Universitario Monte S. Angelo, Via Cintia, I-80126 Napoli, Italy, and Department of Chemistry and Center for Nanoscale Science and Technology, Mail Stop 60, Rice University, Houston, Texas 77005-1892

Received July 12, 2001

Abstract: The structure and magnetic properties of one-dimensional chains of representative nitroxides have been studied by a density functional model employing periodic boundary conditions. The optimized geometries are in better agreement with experiments than those obtained from optimizations of model dimeric systems. The spin populations and isotropic hyperfine couplings compare well with the values measured by polarized neutron and electron spin resonance experiments. Magnetic couplings computed by the broken symmetry approach reproduce the ferro- or antiferromagnetic behavior of different nitroxides derived from experiments. These results point out the reliability of the computational model and the significant tuning of all the magnetic properties by intermolecular hydrogen bridges.

Introduction

The study of the magnetic properties of purely organic materials is attracting an increasing interest, because of its important implications both for fundamental research and for technological applications.[1−3]

Presently, two different classes of organic ferromagnets have been designed. The first class includes conjugated polymers, whose magnetic coupling is ruled by through-bond interactions. In these materials, the radical center can be either a backbone constituent (backbone-type)[4] or a side substituent (pendant-type) of the polymer.[5−7] Alternatively, molecular crystals of stable radicals can be used:[8−13] in this case the magnetic coupling is transmitted via weak intermolecular interactions.[14]

Due to their stability,[15] nitroxides are probably the most used radical centers in both types of organic ferromagnets.[8,16] In the past few years considerable efforts have thus been devoted to design and produce nitroxide-based ferromagnetic materials by finding the chemical modifications that can best tune the magnetic coupling.[17] Theoretical studies can be of big help in elucidating the relationship between structure and magnetic properties,[18,19] especially if they permit the analysis of the

* Corresponding author. E-mail enzo@chemistry.unina.it.
[†] Dipartimento di Chimica, Napoli.
[‡] Department of Chemistry, Houston.

(1) *Molecular Magnetism: From Molecular Assemblies to the Devices;* Coronado, E., Delhaès, P., Gatteschi, D., Miller, J. S., Eds.; NATO Advanced Study Institute Series E321; Kluwer Academic Publishers: Dordrecht, The Netherlands, 1996.
(2) Kahn, O. *Molecular Magnetism*; VCH: New York, 1993.
(3) *Magnetic Molecular Materials*; Gatteschi, D., Kahn, O., Miller, J. S., Palacio, E., Eds.; Kluwer Academic Publishers: Dordrecht, The Netherlands, 1991.
(4) (a) Fujita, I.; Teki, Y.; Takyui, T.; Kinoshita, T.; Itoh, K.; Miko, F.; Sawaki, Y.; Iwamura, H.; Izuoka, A.; Sugawara, T. *J. Am. Chem. Soc.* **1990**, *112*, 4074. (b) Utamapanya, S.; Kakegawa, H.; Bryant, L.; Rajca, A. *Chem. Mater.* **1993**, *5*, 1053. (c) Rajca, A.; Utamapanya, S. *J. Am. Chem. Soc.* **1993**, *115*, 10688.
(5) Nishida, H.; Kaneko, T.; Nii, T.; Katoh, K.; Tsuchida, E.; Lahti, P. M. *J. Am. Chem. Soc.* **1996**, *118*, 9695.
(6) (a) Nishida, H.; Kaneko, T.; Nii, T.; Katoh, K.; Tsuchida, E.; Yamaguchi, K. *J. Am. Chem. Soc.* **1995**, *117*, 548.
(7) Mitani, M.; Yamaki, D.; Yoshioka, Y.; Yamaguchi, K. *J. Chem. Phys.* **1999**, *111*, 2283.
(8) (a) Chiarelli, R.; Novak, M. A.; Rassat, A.; Tholence, J.-L. *Nature* **1993**, *363*, 147. (b) Kinoshita, M.; Turek, P.; Tamura, M.; Nozawa, K.; Shiomi, D.; Nakazawa, Y.; Ishikawa, M.; Takahashi, M.; Awaga, K.; Inabe, T.; Maruyama, Y. *Chem. Lett.* **1991**, 1225. (c) Desiraju, G. R. *Angew. Chem., Int. Ed. Engl.* **1995**, *34*, 2311.
(9) Romero, F. M.; Ziessel, R.; Bonnet, M.; Pontillon, Y.; Ressouche, E.; Schweizer, J.; Delley, B.; Grand, A.; Paulsen, C. *J. Am. Chem. Soc.* **2000**, *122*, 1298.
(10) Maruta, G.; Takeda, S.; Imachi, R.; Ishida, T.; Nogami, T.; Yamaguchi, K. *J. Am. Chem. Soc.* **1999**, *121*, 424.
(11) Nogami, T.; Ishida, T.; Yasui, M.; Iwasaki, F.; Iwamura, H.; Takeda, N.; Ishikawa, M. *Mol. Cryst. Liq. Cryst.* **1996**, *279*, 29.
(12) Lemaire, H.; Rey, P.; Rassat, A.; De Combarieu A.; Michel, J. C. *Mol. Phys.* **1968**, *14*, 201.
(13) Kumano, M.; Ikegami, Y. *Chem. Phys. Lett.* **1978**, *54*, 109.
(14) (a) Cirujeda, J.; Hernaández-Gasió, E.; Rovira, C.; Stanger, J. L.; Turek, P.; Veciana, J. *J. Mater. Chem.* **1995**, *5*, 243. (b) Kawakami, T.; Takeda, S.; Mori, W.; Yamaguchi, K. *Chem. Phys. Lett.* **1996**, *261*, 129.
(15) (a) *Spin Labeling: Theory and Applications*; Berliner, L. G., Ed.; Academic Press: New York, 1976. (b) Rassat, A. *Pure Appl. Chem.* **1990**, *62* 223.
(16) (a) Mito, M.; Kawae, T.; Hitaka, M.; Takeda, K.; Ishida, T.; Nogami, T. *Chem. Phys. Lett* **2001**, *333*, 69. (b) Nogami, T.; Tomioka, K.; Ishida, T.; Yoshikawa, K.; Yasui, M.; Iwasaki, F.; Iwamura, H.; Takeda, N.; Ishikawa, M. *Chem. Lett.* **1994**, 29. (c) Sugawara, T.; Matsushita, M. M.; Izuoka, A.; Wada, N.; Takeda, N.; Ishikawa, M. *J. Chem. Soc., Chem. Commun.* **1994**, 1723.
(17) (a) Desiraju, G. R. *Chem. Commun.* **1997**, 1475. (b) Caneschi, A.; Ferraro, F.; Gatteschi, D.; Le Lirzin, L.; Novak, M.; Rentschler, E.; Sessoli, R. *Adv. Mater.* **1996**, *8*, 826. (c) Romero, F. M.; Ziessel, R.; Drillon, M.; Tholence, J.-L.; Paulsen, C.; Kyritsakas, N.; Fischer, J. *Adv. Mater.* **1996**, *8*, 826.
(18) (a) Barone, V.; Bencini, A.; Di Matteo A. *J. Am. Chem. Soc.* **1997**, *119*, 10831. (b) Adamo, C.; Subra, R.; di Matteo, A.; Barone, V. *J. Chem. Phys.* **1998**, *109*, 10244. (c) Barone, V.; Bencini, A.; Cossi, M.; Di Matteo, A.; Mattesini, M.; Totti, F.; *J. Am. Chem. Soc.* **1998**, *120*, 7069. (d) Di Matteo, A.; Barone, V. *J. Phys. Chem. A* **1999**, *103*, 7676. (e) Improta, R.; Scalmani, G.; Barone, V. *Chem. Phys. Lett.* **2001**, *336*, 349.

magnetic centers in condensed phases.[18,20] The equilibrium between ferromagnetic and antiferromagnetic coupling is very delicate: it strongly depends on the balance among many different types of interactions (both intra- and intermolecular), and on the molecular arrangement in the crystal. Neglecting all the long-range effects due to the crystal field can thus be very dangerous and, for some systems, can prevent obtaining meaningful results.

This is indeed the case for some nitroxide crystals, where the molecules are connected by a hydrogen-bond network (involving the NO moiety). The latter is believed to play a fundamental role in the transmission of magnetic coupling.[9,10,14] Each nitroxide group is hydrogen-bonded, and thus all the magnetic orbitals are perfectly equivalent. This feature cannot be reproduced if a single dimer is taken into account: in this case only one of the NO moieties is hydrogen-bonded, breaking the symmetry and introducing a bias into the description of the magnetic features of the nitroxide, even if the experimental geometry (with two equivalent nitroxide molecules) is used in the calculations.

Proper use of the periodic boundary conditions (hereafter PBC) is thus of overwhelming importance[20] in the study of such species. Furthermore, several works have shown that computational models based on the density functional theory (DFT) are particularly suitable for the analysis of the structure and magnetic properties of open shell species.[18,21] In this contribution we resort to a new PBC/DFT approach, which enables geometry optimizations with large Gaussian basis sets and yields interesting results when applied to several different chemical systems, from nanotubes to biopolymers.[22,23] This method is applied here to the study of three nitroxide derivatives: 2,2,6,6-tetramethylpiperidin-1-oxyl (hereafter Tempo) and its 4-hydroxy (hereafter HO-Tempo) and 4-hydroxyimino (hereafter HON-Tempo) derivatives. Both HO-Tempo and HON-Tempo are six-membered cyclic nitroxides with a para electron-withdrawing group, and both of them exhibit intermolecular OH−ON hydrogen bonds in the solid state. Despite their similarity, the molecular crystals of these two nixtroxides exhibit opposite magnetic features: HO-Tempo is antiferromagnetic,[12,13] whereas HON-Tempo is ferromagnetic.[10,11] A theoretical analysis can contribute to the explanation of such a difference, providing useful insights about the different effects governing the magnetic features of nitroxide molecular crystals.

Furthermore, the comparison between the results obtained for HO-Tempo and Tempo (that cannot form intermolecular hydrogen bonds in the crystal) can assess the role of hydrogen-bond networks in determining the transmission of magnetic interactions in crystals.

2. Theoretical Background

2.1. Magnetic Coupling Exchange Constant. The Heisenberg−Dirac-VanVleck (HDV)[24] spin Hamiltonian is usually used for describing the magnetic interaction between paramagnetic centers. When considering only the interactions between nearest neighbors, it reduces to

$$\hat{H} = -\sum_{\langle i,j \rangle} J_{ij} \hat{S}_i \hat{S}_j \tag{1}$$

where the symbol $\langle i,j \rangle$ indicates that the summation runs just over the neighbor centers, $\hat{S}_i$ and $\hat{S}_j$ are the total spin operators for magnetic centers i and j, and J_{ij} is the so-called magnetic coupling constant between them, related to the energy difference between the eigenstates of the HDV Hamiltonian which are pure spin eigenfunctions. For example, in the case of two particles with $S = {}^1/_2$,

$$J = E(S) - E(T) \tag{2}$$

where S and T stay for singlet and triplet, respectively.

In many cases, including the periodic systems we are examining, finding the eigenfunctions of the HDV Hamiltonian is not straightforward or even possible. A common approach to such cases relies on the use of a simplified version of the HDV Hamiltonian, the Ising Hamiltonian[25−27] (H^{I}), where total spin operators are substituted by their z-components. Equation 1 thus reduces to:

$$\hat{H}^{\mathrm{I}} = -\sum_{\langle i,j \rangle} J_{ij} \hat{S}_{z,i} \hat{S}_{z,j} \tag{3}$$

The eigenfunctions of H^{I} are not always eigenfunctions of $\hat{S}^2$, but, since H^{I} commutes with S_z, M_s is still a good quantum number. The Ising Hamiltonian can thus be easily connected to all the unrestricted formalisms based on a single-determinant approach (either Hartree−Fock or Kohn−Sham−Slater). In these cases, J can always be obtained from the energy of the states with maximum and minimum M_s, the so-called ferromagnetic (FM) and antiferromagnetic (AFM) states, respectively.

In an unrestricted single determinant approach, only the ferromagnetic state can always be a spin eigenfunction (when neglecting spin contaminations). Following Noodleman,[28] the antiferromagnetic state can instead be described by a broken symmetry (BS) determinant. For two particles with $S = {}^1/_2$, the BS state is built by imposing a localization of the spin on each

(19) (a) Ruiz, E.; Alemany, P.; Alvarez, S.; Cano, J. *J. Am. Chem. Soc.* **1997**, *119*, 1297. (b) Ruiz, E.; Cano, J.; Alvarez, S.; Alemany, P. *J. Am. Chem. Soc.* **1998**, *120*, 11122. (c) Barone, V.; Bencini, A.; Ciofini, I.; Daul, C.A.; Totti, F. *J. Am. Chem. Soc.* **1998**, *120*, 8357. (d) Adamo, C.; Barone, V.; Bencini, A.; Totti, F.; Ciofini, I. *Inorg. Chem.* **1999**, *38*, 1996. (e) Adamo, C.; Barone, V.; Subra, R. *Theor. Chem. Acc.* **2000**, *104*, 207.
(20) (a) Ricart, J. M.; Dovesi, R.; Roetti, C.; Saunders: V. R. *Phys. Rev. B* **1995**, *52*, 2381. (b) Reinhardt, P.; Habas, M. P.; Dovesi, R.; de P. R. Moreira I; Illas F. *Phys. Rev. B* **1999**, *59*, 1016.
(21) (a) Barone, V. In *Recent Advances in Density Functional Methods*; Chong, D. P., Ed.; World Scientific: Singapore, 1995; p 287. (b) Barone, V.; di Matteo, A.; Mele, F.; de P. R. Moreira, I.; Illas, F. *Chem. Phys. Lett.* **1999** *302*, 240. (c) Adamo, C.; di Matteo, A.; Rey, P.; Barone, V. *J. Phys. Chem. A* **1999** *103*, 3481. (d) di Matteo, A.; Adamo, C.; Cossi, M.; Barone, V.; Rey, P. *Chem. Phys. Lett.* **1999** *310*, 159. (e) Improta, R.; di Matteo, A.; Barone, V. *Theor. Chem. Acc.* **2000** *104*, 273.
(22) (a) Kudin, K. N.; Scuseria, G. E. *Chem. Phys. Lett.* **1998**, *289*, 611. (b) Kudin, K. N.; Scuseria, G. E. *Chem. Phys. Lett.* **1998**, *283*, 61. (c) Kudin, K. N.; Scuseria, G. E. *J. Chem. Phys.* **1999**, *111*, 2351. (d) Kudin, K. N.; Scuseria, G. E. *Phys. Rev. B* **2000**, *61*, 5141.
(23) (a) Improta, R.; Barone, V.; Kudin, K. N.; Scuseria, G. E. *J. Am. Chem. Soc* **2001**, *123*, 3311. (b) Improta, R.; Barone, V.; Kudin, K. N.; Scuseria, G. E. *J. Chem. Phys* **2001**, *114*, 2541. (c) Kudin, K. N.; Scuseria, G. E. *Phys. Rev. B* **2000** , *61*, 16440. (d) Kudin, K. N.; Bettinger H. F.; Scuseria, G. E. *Phys. Rev. B* **2001** , *6304*, 5413. (e) Bettinger, H. F.; Kudin, K. N.; Scuseria, G. E. *J. Am. Chem. Soc.* In press. (f) Kudin, K. N.; Scuseria, G. E.; Yakobson, B. I. *Phys. Rev. B* Manuscript submitted.
(24) (a) Heisenberg, W. Z. *Z. Phys.* **1928**, *49* 619. (b) Dirac, P. A. *Proc. R. Soc.* **1929**, *A123* 714. (c) van Vleck, J. H. *The Theory of Electric and Magnetic Susceptibility*; Oxford University Press: London, 1932.
(25) (a) Bonner, J. C.; Fisher, M. E. *Phys. Rev. A* **1964**, *135*, 640. (b) Dixon, J. M.; Tuszynski, J. A.; Nip, M. L. A. *Physica A* **2001**, *289*, 137.
(26) de P. R. Moreira I; Illas F. *Phys. Rev. B* **1997**, *55*, 4129.
(27) Illas, F.; de P. R. Moreira I; de Graaf, C.; Barone, V. *Theor. Chem. Acc.* **2000**, *104*, 265.
(28) (a) Noodleman, L. *J. Chem. Phys.* **1981**, *74*, 5737. (b) Noodleman, L. *Adv. Inorg. Chem.* **1992**, *38*, 423.

magnetic center and a global antiparallel alignment between the spins of the (two) interacting centers.[28,29]

Using the broken symmetry approach and a recently developed quite general formalism,[30] J can be calculated according to eq 4

$$J = \frac{(E_{BS} - E_T)}{1 - b^2} \tag{4}$$

where

$$b^2 = \frac{1}{2}\langle\psi_{BS}|\,\hat{S}^2|\psi_{BS}\rangle \tag{5}$$

and E_{BS}, E_T are the energies of the broken symmetry (ψ_{BS}) and of the triplet state, respectively.

When dealing with infinite polymers, it is necessary to take into account that each magnetic center can have more than one nearest neighbor: assuming additivity of two-body interactions,[21] eq 5 becomes

$$J = \frac{(E_{BS} - E_T)}{(1 - b^2)z} \tag{6}$$

where z, is the number of nearest neigbors of each nitroxide. Since in the systems we studied $z = 2$, and the BS states always have $\langle\psi_{BS}|\,\hat{S}^2|\psi_{BS}\rangle$ extremely close to 1, the magnetic coupling is simply

$$J = E_{BS} - E_T \tag{7}$$

We have calculated the energy of the triplet state by using a cell containing two nitroxides and imposing a triplet spin multiplicity. Then E_{BS} has been calculated by using the same doubled cell, starting from the triplet wave function, with its highest occupied (HOMO) and lowest unoccupied (LUMO) molecular orbitals mixed.

Finally, it is worth highlighting that in the systems under study the magnetic coupling is expected to be strongly anisotropic. It is then possible to compare computational results calculated by the Ising Hamiltonian with experimental data fitted according to the Heisenberg Hamiltonian.

3. Computational Details

All calculations were performed with the help of a development version of the Gaussian program.[31] The implementation of PBC/DFT in the above program is described in ref 22 and is extended in the present work to open-shell systems. On the ground of previous experience, most computations have been performed by using the PBE density functional,[32] whose accuracy is well documented for a wide variety of systems including hydrogen bonds.[23,33]

Geometry optimizations of periodic systems were carried out by a new redundant internal coordinate algorithm,[34] which optimizes simultaneously atomic positions and lattice dimensions.[35] The molecular crystals formed by TEMPO derivatives have large translational vectors and substantial band gaps, and therefore 8 **k** points were sufficient to converge energy and forces with very high accuracy. Geometry optimizations have been performed with the 6-31G(d) basis set[36] on repeating cells containing one nitroxide molecule. The effects of the basis set size and of the specific functional form have then been investigated by single-point calculations with the 6-31+G(d,p) basis set,[36] and with the BLYP[37] and PBE0[38] functionals. In the last case, the Hartree−Fock exchange contribution was computed within the region that includes the central cell and its first neighbors. A more detailed description of the hybrid functional results as well as a benchmark comparison of different methods will be given in ref 39.

The isotropic hyperfine coupling constant (hcc) of each nucleus (N) has been obtained by using the following formula[40,41]

$$A_N = \frac{8}{3}\pi g_n g_e \mu_n \mu_e \rho_s(r_N) \tag{8}$$

where $\rho_s(r_N)$ is the electronic spin density at the nucleus. In eq 2 μ_e is the Bohr magneton, g_e is the g value for the electron (in the present

Table 1. Selected Geometrical Parameters Calculated at the PBE/6-31G(d) Level for HO-Tempo in Different Molecular Environments Are Compared with the Available Experimental Results

	exp[a]	1D chain	dimer[b]	dimer[c]	monomer
N1−O1	1.291	1.293	1.293	1.290	1.290
C2−N1	1.498	1.509	1.508	1.508	1.508
C3−C2	1.526	1.544	1.545	1.543	1.543
C4−C3	1.517	1.533	1.532	1.533	1.531
C4−O2	1.422	1.423	1.430	1.428	1.431
O2−H2	0.89	0.995	0.981	0.994	0.981
C6−N1−C3	125.4	124.7	124.2	124.1	124.0
N1−C2−C3	110.1	110.0	109.4	110.5	110.3
C2−C3−C4	113.1	113.6	114.1	114.2	114.2
O2−C4−C3	112.3	112.5	111.9	111.7	111.9
τ	15.8	16.7	18.1	22.1	22.5
O1−N1−C2−C3	−167.5	−165.5	−162.6	−171.2	−170.5
N1−C2−C3−C4	44.6	45.6	46.2	46.2	45.4
O2−C4−C3−C2	173.3	174.4	177.3	177.4	177.2
H1−O2−C4−C3	61.1	61.3	60.0	61.5	61.2
O1−H1′	1.99	1.823	1.80		
O1−O2′	2.82	2.79	2.79		
O1−H1′−O2′		163.0	174.1		
N1−O1−H1′	124.0	115.6	113.7		
N1−O1−O2′	116	109.6	112.5		
O1−O2′−C4	120	120.0	110.2		
N1−O1−H1′−O2′		0.0	−0.9		

[a] Reference 42. [b] H-bond acceptor. [c] H-bond donor. [d] Energy (in au): dimer in 1D chain (PBC/PBE/6-31G(d) optimization) = −1116.47044; insulated dimer (PBE/6-31G(d) optimization) = −1116.45487; insulated monomer (PBE/6-31G(d) optimization) = −558.21904.

(29) (a) Caballol, R.; Castell, O.; Illas, F.; Moreira, P. R.; Malrieu, J. P. *J. Phys. Chem.* **1997**, *101*, 7860.
(30) (a) Ovchinnikov, A.; Labanowski, J. K. *Phys. Rev. A* **1996**, *53*, 3946. (b) Barone, V.; Bencini A.; Ciofini I.; Daul C. *J. Phys. Chem. A* **1999**, *103*, 4275.
(31) Frisch, M. J.; Trucks, G. W.; Schlegel, H. B.; Scuseria, G. E.; Robb, M. A.; Cheeseman, J. R.; Zakrzewski, V. G.; Montgomery, J. A., Jr.; Stratmann, R. E.; Burant, J. C.; Dapprich, S.; Millam, J. M.; Daniels, A. D.; Kudin, K. N.; Strain, M. C.; Farkas, O.; Tomasi, J.; Barone, V.; Mennucci, B.; Cossi, M.; Adamo, C.; Jaramillo, J.; Cammi, R.; Pomelli, C.; Ochterski, J.; Petersson, G. A.; Ayala, P. Y.; Morokuma, K.; Malick, D. K.; Rabuck, A. D.; Raghavachari, K.; Foresman, J. B.; Ortiz, J. V.; Cui, Q.; Baboul, A. G.; Clifford, S.; Cioslowski, J.; Stefanov, B. B.; Liu, G.; Liashenko, A.; Piskorz, P.; Komaromi, I.; Gomperts, R.; Martin, R. L.; Fox, D. J.; Keith, T.; Al-Laham, M. A.; Peng, C. Y.; Nanayakkara, A.; Challacombe, M.; Gill, P. M. W.; Johnson, B.; Chen, W.; Wong, M. W.; Andres, J. L.: Gonzalez, C.; Head-Gordon, M.; Replogle, E. S.; Pople, J. A. *Gaussian 99*, Development Version, revision C.01; Gaussian, Inc.: Pittsburgh, PA, 2000.
(32) Perdew, J. P.; Burke, K.; Ernzerhof, M. *Phys. Rev. Lett.* **1996**, *77*, 3865; Perdew, J. P.; Burke, K.; Ernzerhof, M. *Phys. Rev. Lett. (E)* **1997** *78*, 1396.
(33) (a) Rabuck, A. D.; Scuseria, G. E. *Chem. Phys. Lett* **1999** *309*, 450. (b) Rabuck, A. D.; Scuseria, G. E. *Theor. Chem. Acc.* **2000**, *104*, 439.
(34) Peng, C.; Ayala, P. Y.; Schlegel, H. B.; Frisch, M. J. *J. Comput. Chem.* **1996**, *17*, 49.
(35) Kudin, K. N.; Scuseria, G. E.; Schlegel, H. B. *J. Chem. Phys* **2001**, *114*, 2919.
(36) A description of basis sets and standard computational methods can be found in: Foresman, J. B.; Frisch, A. E. *Exploring Chemistry with Electronic Structure Methods*, 2nd ed.; Gaussian Inc.: Pittsburgh, PA 1996.
(37) (a) Becke, A. D. *Phys. Rev. A* **1988**, *38*, 3098. (b) Lee, C.; Yang, W.; Parr, R. G. *Phys. Rev. B* **1987**, *37*, 785.
(38) (a) Enzerhof, M.; Scuseria, G. E. *J. Chem. Phys.* **1999**, *110*, 5029. (b) Adamo, C.; Barone, V. *J. Chem. Phys.* **1999**, *110*, 6158.
(39) Improta, R.; Barone, V.; Kudin, K. N.; Heyd, J.; Scuseria, G. E. In preparation

Table 2. Selected Geometrical Parameters Calculated at the PBE/6-31G(d) Level for HON-Tempo in Different Molecular Environments Are Compared with the Available Experimental Results

	exp[a]	1D chain	dimer[a]	dimer[b]	monomer
N1−O1	1.28	1.295	1.295	1.289	1.289
C2−N1	1.49	1.510	1.507	1.511	1.511
C3−C2	1.53	1.550	1.551	1.550	1.552
C4−C3	1.50	1.503	1.502	1.502	1.500
C4−C5	1.57	1.500	1.500	1.500	1.502
C4−N2	1.28	1.297	1.295	1.297	1.294
N2−O2	1.38	1.398	1.419	1.397	1.419
O2−H2		1.000	0.979	1.001	0.979
C6−N1−C3	125	125.5	124.7	124.2	124.3
N1−C2−C3	111	109.8	109.2	110.1	110.1
C2−C3−C4	111	110.2	110.8	110.8	111.5
C5−C4−C3	116	113.8	114.2	114.1	114.1
N2−C4−C3	133	127.4	127.9	127.4	127.9
O2−N2−C4	111	112.6	111.8	113.1	111.8
τ	26.2	21.7	18.32	23.5	23.3
O1−N1−C2−C6	−151.2	−155.9	−159.5	−153.9	−154.1
O1−N1−C2−C3	168.9	169.6	160.8	169.0	169.1
N1−C2−C3−C4	42.5	45.2	46.2	45.1	45.1
N2−C4−C3−C2	128.5	110.5	116.3	115.7	116.3
O2−N2−C4−C3	3.4	3.3	1.55	1.74	1.48
H1−O2−N2−C4		−174.4	178.6	179.8	178.8
O1−H1′		1.714		1.75	
O1−O2′	2.74	2.71		2.75	
N1−O1−H1′		117.8			
O1−H1′−O2′		176.0			
N1−O1−O2′	130	119.3		98.3	
N1−O1−H1′−O2′		173.4		2.72	
O1−H1′−O2′−N2′		85.1		−14.8	

[a] Reference 44. [b] H-bond acceptor. [c] H-bond donor. [d] Energy (in au): dimer in 1D chain (PBC/PBE/6-31G(d) optimization) = −1224.57725; dimer in 1D chain (PBC/PBE/6-31+G(d,p) single point) = −1224.67601; dimer in 1D chain (PBC/BLYP/6-31G(d) single point) = −1224.54776; insulated dimer (PBE/6-31G(d) optimization) = −1224.56443; insulated monomer (PBE/6-31G(d) optimization) = −612.27342.

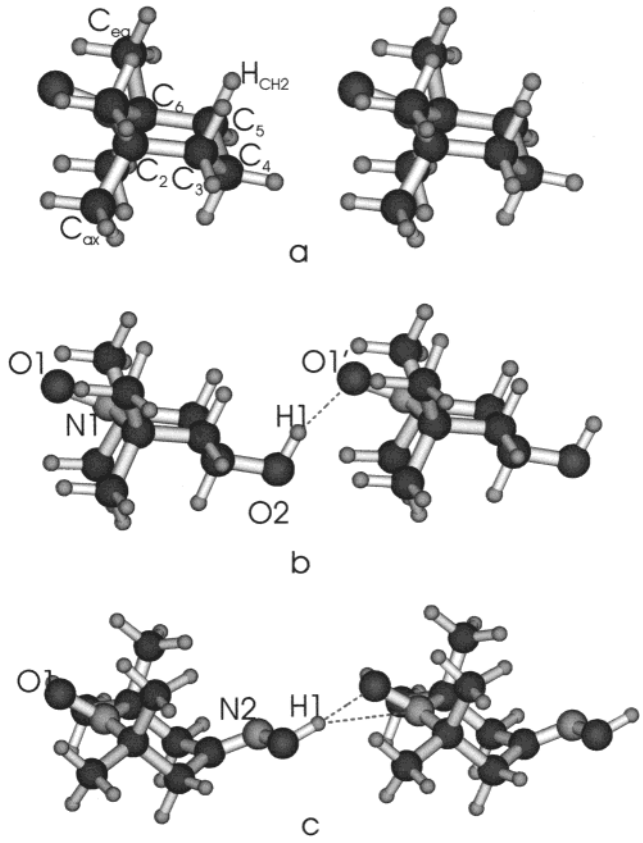

Figure 1. Atom labeling and optimized geometry (PBC PBE/6-31G(d) calculations) of dimers belonging to infinite 1D chains for Tempo (a), HO-Tempo (b), and HON-Tempo (c).

work it has been taken equal to 2.0) and μ_n, g_n are the nuclear magneton and nuclear g factors, respectively. All our results are given in MHz. To convert them to Gauss one has to divide by 2.8025.

4. Results

In the crystals of HO-Tempo and HON-Tempo each hydroxyl/hydroxymino group is hydrogen-bonded to the NO group of an adjacent molecule forming an 1D infinite chain. Nitroxides belonging to different 1D chains can further interact through CH_3-ON or CH_3-CH_3 contacts.[42−44] However, since these van der Waals interactions are expected to be rather weak (C−O and C−C distances in the range 3.3−3.7 Å), the hydrogen bond interaction is likely to dominate the transmission of the magnetic coupling in the crystals. We then focus our attention on the latter interaction, and all the PBC results refer to one-dimensional hydrogen-bonded chains neglecting all interchain contacts.

4.1. Structures. Inspection of Tables 1 and 2 shows that the geometries of HO-Tempo and HON-Tempo optimized at the PBC/PBE/6-31G(d) level (see Figure 1) are in good agreement with experimental X-ray structures.[42−44] The calculated bond lengths show maximum errors of ∼1% with respect to the experimental values and the agreement between experimental and calculated bond angles is even better. The ring conformations and the piramidality of the NO moieties optimized by the PBC method are similar to their experimental counterparts for both nitroxides. This is a remarkable result, since the magnetic properties of nitroxides strongly depend on the degree of pyramidalization of the nitrogen atom, that can be measured by the angle between the NO bond and the C2NC6 plane (τ).

Tables 1−2 collect also the results of the PBE/6-31G(d) geometry optimization performed on the "insulated" H-bonded dimers and on the monomers. It is worth noting that the results of the PBC optimizations are usually closer to the crystallographic structure, with bonds and dihedral angles matching the best. The few exceptions are found in HON-Tempo; the value of the NO bond length optimized for the monomer is, for example, closer than the PBC one to the value predicted by X-ray experiments. However, the experimental value of 1.28 Å seems to be uncertain in itself, because the NO group is involved in an intermolecular hydrogen bond. Overall, the main drawback of the dimer optimizations is that the two nitroxides are no more equivalent. Moreover, while the relative orientation of the two HO-Tempo molecules is very similar to that found in the crystals (coaxial NO bond), for HON-Tempo the crystal symmetry is completely broken (see Figure 2).

4.2. Spin Populations. Since the singly occupied molecular orbital (SOMO) is strongly concentrated on the nitroxide moiety, the spin populations of N and O atoms are large and positive (spin delocalization (SD) or direct contribution). In agreement with previous experimental and theoretical studies,[18] this effect accounts for ∼90% of the total spin population, which is almost equally shared between nitrogen and oxygen (vide infra). The much lower spin populatios of the remaining atoms originate

(40) Weltner, W. *Magnetic Atoms and Molecules*; Dover: New York; 1989.
(41) McConnel, H. M.; Chesnut, D. B. *J. Chem. Phys.* **1958**, *28*, 107.
(42) Berliner, L. J. *Acta Crystallogr.* **1970**; *B26*, 1198.
(43) Lajzérowicz-Bonneteau J. *Acta Crystallogr.* **1968**, *B24*, 196.
(44) Bordeaux, D.; Lajzérowicz J. *Acta Crystallogr.* **1977**, *B33*, 1837.

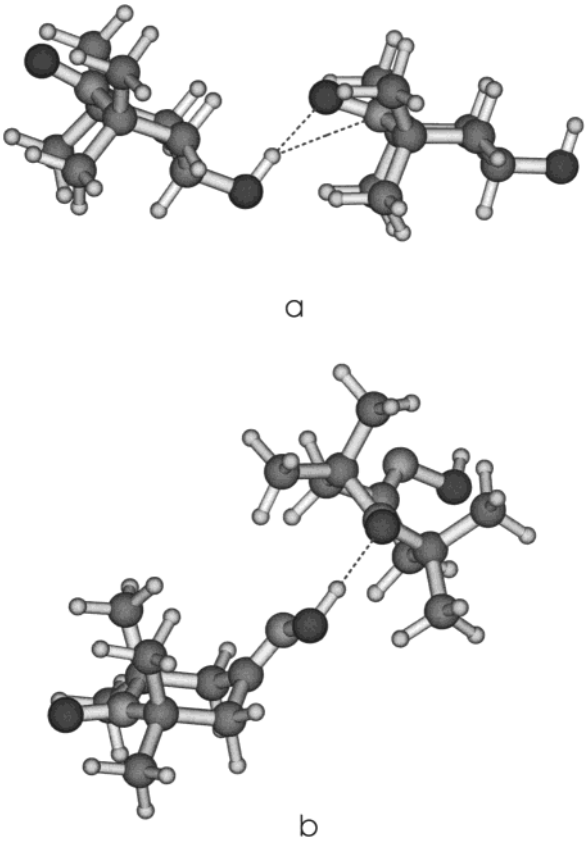

Figure 2. Geometries of HO-Tempo (a) and HON-Tempo dimers optimized at the PBE/6-31G(d) level.

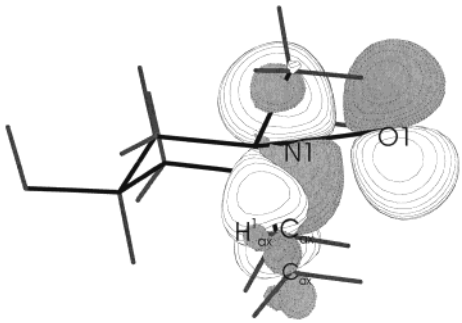

Figure 3. SOMO of HO-Tempo according to unrestricted PBE/6-31G(d) calculations.

Table 3. Mulliken Spin Populations on the Nitroxide Moiety for HO-Tempo and HON-Tempo Issuing from PBE/6-31G(d) Computations

		exp[a]	1D chain	dimer[b]	dimer[c]	monomer
HO−Tempo	N1	0.544	0.495	0.489	0.443	0.440
	O1	0.354	0.420	0.424	0.494	0.497
HON−Tempo	N1		0.500	0.504	0.440	0.439
	O1		0.417	0.409	0.497	0.498

[a] Reference 45. [b] H-bond acceptor. [c] H-bond donor. [d] Results for 1D Tempo: N1 = 0.457 O1 = 0.483. Monomer (same geometry as 1D) N1 = 0.448 O1 = 0.496

Table 4. Hyperfine Coupling Constants (in MHz) of Hydrogen Atoms in HO-Tempo and HON-Tempo

		exp[a]	1D chain	dimer[b]	dimer[c]	monomer
HO−Tempo	H1	−4.48	−4.14	−0.030	−4.02−0.030	−0.026
	H_{CH_2}	−2.24	−0.86	−0.79	−0.98	−0.88
HON−Tempo	H1	−2.93	−4.37	−0.08	−4.54	−0.07
	H_{CH_2}	−1.43	−1.12	−1.10	−1.04	−1.03
	H_{eq}	−1.56	−0.92	−0.92	−1.00	−1.00
	H_{ax}	0.85	1.01	1.10	0.80	0.84

[a] Reference 47. [b] H-bond acceptor. [c] H-bond donor. [e] Reference 10.

from spin polarization (SP). As a matter of fact, the unpaired electron (by convention with α spin) interacts differently with the two electrons of a spin-paired bond, because the exchange interaction is operative only between electrons with parallel spins. This induces an enhancement of α-spin density in the σ orbitals of atoms on which the SOMO is localized and a corresponding increase of β-spin density in the σ orbitals of atoms to which they are directly bonded. This leads, in turn, to accumulation of β-spin density in the π orbitals of these atoms, and so on. As a consequence the carbon atoms of the ring exhibit the damped oscillatory pattern typical of spin polarized chains. C2 and C6 atoms have negative Mulliken spin populations, as is also the case for C4 (much smaller absolute value). C3 and C5 atoms have instead a positive Mulliken spin population. Methyl substituents have positive spin populations, in agreement with the spin alternation rule. However the spin population of axial methyls is four times larger than that of equatorial methyls, in agreement with neutron diffraction studies on HO-Tempo, that predict a ratio of 7 for the spin populations of axial and equatorial methyls.[45] This result clearly shows that the spin population of axial methyls has also a direct contribution to the spin density (see Figure 3). One of the axial methyl hydrogens contributes to the SOMO, and thus has a nonnegligible positive spin population. This can explain why deuterium-NMR experiments on HON-Tempo predict for the axial methyl hydrogens a positive spin population (see also Table 4).[10] Due to the rapid methyl rotation, experiments record an average of the hyperfine coupling constants of methyl hydrogens. All the equatorial hydrogens have a negative spin population, and experiments give a negative average hcc for those atoms. As mentioned above, one of the axial hydrogens has a quite large positive hcc, partially balanced by the small negative contributions of the remaining two hydrogens. Experiments predict indeed a positive hcc, but with a smaller absolute value than the "equatorial" one.

Preliminary PBC/PBE0 calculations[39] yield spin populations very similar to those obtained by the PBE model, but for providing slightly larger spin polarization contributions. This leads to a general better agreement with experiments, mostly for what concerns the carbon atom of the nitroxide ring.

Inspection of Table 3 shows that in the crystal the spin density distribution of the nitroxide (mostly of the NO moiety) is remarkably different from that of the insulated radical.

As a matter of fact, PBE/6-31G(d) calculations performed on the monomer give a Mulliken spin population of 0.440 on the nitrogen and of 0.497 on the oxygen. On the contrary, in the solid state the unpaired electron is more localized on the nitrogen atom than on the oxygen atom of the NO moiety: the Mulliken spin population (PBC PBE/6-31G(d) calculations) of nitrogen is indeed 0.495, whereas that of the oxygen is 0.420. Neutron diffraction experiments give similar indications. In the HO-Tempo crystals, the nitrogen atom has indeed a spin population of 0.544 and the oxygen atom of 0.354.[45] On the other hand, neutron diffraction experiments on di(HO-Tempo)-suberate (where two nitroxides are grafted on a suberic acid moiety) show that the spin population is nearly equally

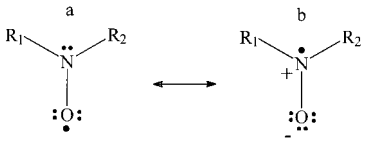

Figure 4. The two most important resonance structures of the nitroxide moiety.

partitioned between oxygen and nitrogen atoms, with a slightly larger contribution of oxygen.[46−48]

In HO-tempo and HON-Tempo each NO moiety is involved in intermolecular hydrogen bonds, at variance with di(HO-Tempo)suberate. The presence of a hydrogen bond makes the ionic resonance structure of the NO moiety relatively favored over the covalent one (see Figure 4), increasing the nitrogen spin population and decreasing the oxygen one. As a matter of fact, in the dimers of HO-Tempo and of HON-Tempo the H-bond acceptor NO group exhibits a spin distribution similar to that found in the crystal. To better understand the role of environmental effects (other than hydrogen bonds) in tuning the NO spin density, we performed PBC PBE/6-31G(d) calculations on a one-dimensional chain of Tempo, frozen in the same geometry optimized for HO-Tempo at the same level of theory. Despite the absence of hydrogen-bond interactions (in Tempo the OH group is substituted by a hydrogen atom), when inserted in the crystal Tempo also exhibits a spin density distribution slightly different from that of the insulated molecule. The NO group in the crystal has a head-to-tail arrangement that favors the ionic resonance structure sketched in Figure 4. This effect can probably give account of the small shift of spin density from oxygen to nitrogen in the crystal. Test calculations perfomed on different arrangment of a H_2NO dimer (not exhibiting hydrogen bonds) support this picture.

Finally, it is worth noting that the Mulliken spin populations of the HO-Tempo and HON-Tempo monomers are very similar to those predicted by the natural bond orbitals method,[48] (on the basis of the PBE/6-31G(d) wave function) confirming the reliability of the population analysis we used.

4.3. Magnetic Coupling. PBC calculations predict that HO-Tempo crystal is sligthly antiferromagnetic, in agreement with the experiments. The absolute value of the magnetic coupling constant computed in this work is underestimated with respect to the experimental value (−0.96 and −2.9 cm^{-1}, respectively). This discrepancy could be due to a slight overestimation of the hydrogen-bond strength in PBC calculation on HO-Tempo, leading to an overestimation of σ-spin polarization and to a consequent reduction of the antiferromagnetic coupling (vide infra). The small differences between the experimental and the calculated geometry do not significantly affect *J* instead. PBC PBE/6-31G(d) calculations performed by using the experimental geometry of HO-Tempo crystals provide indeed for *J* a value of -1.02 cm^{-1}.

Our calculations confirm the importance of hydrogen-bond chains (OH−ON hydrogen bond in the compound studied) in transmitting magnetic interactions. PBC calculations on Tempo (by using the same procedure outlined above) predict that the magnetic coupling is extremely small ($\sim$0.04 cm^{-1}), suggesting that an effective magnetic coupling requires an intermolecular hydrogen bond, whereas direct through space interactions between the NO moieties are negligible.

Table 5. Experimental Magnetic Couplings *J* (in cm^{-1}) Are Compared with the Results of PBC Calculations at Different Levels of Theory

	PBE[a]		PBE0[a,b]	BLYP[a]	
	6-31G(d)	6-31+G(d,p)	6-31G(d)	6-31G(d)	exp
HON−Tempo	+0.26	+0.16	+0.26	+0.24	+0.44[c]
HO−Tempo	−0.92		−0.11		−2.8[d]
Tempo	+0.04				

[a] PBC PBE/6-31G(d) geometry. [b] Reference 39. [c] Reference 11. [d] Reference 12.

PBC calculations predict instead that HON-Tempo exhibits a ferromagnetic behavior, in agreement with the experimental results. The *J* value issuing from PBC PBE/6-31G(d) calculations is in fair agreement with the experimental result. *J* value quite close to the experimentally determined one (0.26 vs 0.44 cm^{-1}).

To check whether our results depend on the functional and the basis set used in the PBC calculations we have calculated the magnetic coupling for HON-Tempo both at the BLYP/6-31G(d) and at the PBE/6-31+G(d,p) levels, using the PBE/6-31G(d) geometries. The results are very similar to those obtained at the PBE/6-31G(d) level: HON-Tempo is ferromagnetic and *J* is $\sim$0.20 cm^{-1}.

The *J* values calculated by the PBE0/6-31G(d) computational model[39] are in qualitative agreement with those obtained at the PBE level; HON-Tempo PBE0 and PBE calculations predict the same value for *J*. HO-Tempo is predicted to be antiferromagnetic also by the PBE0 model, but the absolute value of *J* is significantly reduced.

4.4. Effects Determining the Different Magnetic Behavior of Nitroxides. It is now interesting to determine the reasons for the different behavior of HO-Tempo and HON-Tempo. As a first step, it is instructive to compare the results obtained at the unrestricted level and at the restricted open-shell level. Restricted open- shell calculations can indeed give useful insights on the weights of the direct contribution to the spin density, since they do not take the spin polarization contribution into account. Direct SOMO−SOMO overlap gives an antiferromagnetic contribution to the magnetic coupling. So it can be expected that an increase of the SD contribution to the (very small) spin population of the hydrogen atom involved in the intermolecular hydrogen bond (H1) stabilizes antiferromagnetic states. The results in Tables 5 and 6 show indeed that the SD contribution to the H1 spin population is slightly larger for HO-Tempo, already at the monomer stage. In other words, H1 contributes more to the SOMO orbital in HO-Tempo than in HON-Tempo. Calculations performed for the triplet electronic state of a dimer can instead provide useful insights on the nature of the intermolecular magnetic interactions. Our calculations predict that the direct SOMO−SOMO interaction is more important for HO-Tempo than for HON-Tempo, explaining the antiferromagnetic behavior of the former compound.

The large reduction of the *J* value predicted by PBE0 calculations confirms this picture. Due to the presence of some

(45) Bordeaux, D.; Boucherle, J. X.; Delley, B.; Gillon, B.; Ressouche, E.; Schweizer, J. *Z. Naturfosch.* **1993**, *48a*, 117.
(46) Brown, P. J.; Capiomont, A.; Gillon, B.; Schweizer J. *Mol. Phys.* **1983**, *48*, 753.
(47) Alonso, A.; Nascimento, O. R.; Tabak, M. *Nuovo Cim. D* **1987**, *9*, 227.
(48) (a) Foster, J. P., Weinhold, F. *J. Am. Chem. Soc.* **1980**, *102*, 7211. (b) Reed, A.; Weinhold, F. *J. Chem. Phys.* **1983**, *78*, 4066. (c) Glendening, E. D.; Weinhold, F. *J. Comput. Chem.* **1998**, *19*, 593.

Table 6. Mulliken Spin Populations of Selected Atoms in HO-Tempo and HON-Tempo[a]

		dimer	dimer RO	monomer	monomer RO
HO−Tempo	N1	0.490	0.440	0.446	0.403
	O1	0.425	0.414	0.498	0.486
	O2′	0.016	0.014	<0.001	< 0.001
	H1′	0.011	0.015	∼0.0	< 0.001
HON−Tempo	N1	0.492	0.442	0.444	0.401
	O1	0.424	0.412	0.497	0.484
	N2′	0.003	0.003	0.004	0.002
	O2′	0.018	0.016	0.001	0.001
	H1′	0.003	0.008	∼0.0	∼0.0

[a] Dimer results refer to triplet electronic states.

Hartree−Fock exchange, hybrid functionals usually provide a larger spin polarization compared to the corresponding conventional functionals. Due to the alternation of spin polarization in the nitroxide, this effect would lead to a negative spin density on H1, counterbalancing part of the direct positive contribution on this atom and decreasing the antiferromagnetic ordering of HO-Tempo crystals.

Unrestricted calculations performed on the HON-Tempo monomer show a strong α-spin population on the NO moiety and a slight accumulation of β-spin population on H1. In this compound the O2−N2 π^* bond gives a nonnegligible contribution to the SOMO, with a quite substantial direct contribution to the N and O spin populations. As we have already seen, the direct contribution is instead negligible for H1. The sum of these two factors results in a negative spin population on H1. Since, as we have seen, direct contributions are less important for HON-Tempo also in the intermolecular coupling, in this compound alternated spin-polarized networks become possible, which explain its ferromagnetic behavior.

5. Discussion and Concluding Remarks

To the best of our knowledge, this is one of the first studies in which periodic geometry optimizations have been applied to the analysis of the magnetic behavior of molecular crystals. The optimized geometries are in good agreement with X-ray experiments, supporting the reliability of the adopted methodology. Moreover, our assumption of considering only one-dimensional H-bonded chains, neglecting interchain contacts appears to be correct and should not affect the reliability of our conclusions.

As expected, geometry optimizations of isolated dimers yield geometries quite different from the experimental ones. Furthermore, even using the experimental geometries would bias the determination of the magnetic properties, since in a hydrogen-bond dimer the NO moieties are no longer equivalent. In the systems we studied, the use of a method capable of taking into account the periodic nature of the crystal seems thus necessary.

The spin populations and the hyperfine coupling constants calculated at the PBC PBE/6-31G(d) level are also in agreement with the available experimental results, showing that a direct comparison is becoming possible between calculations and experiments performed in the solid state. The presence of the crystalline environment affects the magnetic properties of the NO moiety in two ways. The formation of intermolecular hydrogen bonds is the most important factor. Long-range dipolar interactions have a small but noticeable influence on the distribution of the spin density in the NO moiety. In the cases under study, the arrangement of NO dipole should favor ionic resonance structures, increasing the spin population of the nitrogen atom.

Our calculations give a description of the magnetic properties of different nitroxides in agreement with experiments: HO-Tempo crystal is predicted to be antiferromagnetic, and HON-Tempo, crystal ferromagnetic. In the former compound the hydrogen atom involved in the hydrogen bond gives a nonvanishing contribution to the SOMO of the nitroxide. Furthermore, in HO-Tempo the transmission of the magnetic coupling through the H-bond has a larger direct contribution than in HON-Tempo. This is probably due to the fact that the NO and the O1′−H1′ bonds form an angle closer to 90° in HO-Tempo than in HON-Tempo (see Figure 1), causing a larger overlap between the O1′−H1′ orbitals and the NO π system (and thus the SOMO) of the other nitroxide (belonging to the hydrogen-bonded pair). In HO-Tempo the magnetic coupling is thus due mainly to a direct SOMO−SOMO interaction, mediated by the HO group involved in the hydrogen bond. This gives account of the antiferomagnetic behavior of this crystal.

On the other hand, in HON-Tempo, the H1 atom does not contribute to the nitroxide SOMO, while O2 and N2 atoms receive a non negligible "direct" positive contribution to the spin density. As a consequence, H1 has a negative spin density, due to a spin polarization mechanism. Moreover, the hydrogen bond does not imply a significant coupling between the SOMOs of the two nitroxides, partly due to the different geometry of the hydrogen bond and to the vanishing contibution of H1 to the nitroxides's SOMO. All of these effects explain the weak ferromagnetism of HON-Tempo.

Shortly, we can say that in the case of hydrogen-bonded molecular crystals the magnetic behavior is due the subtle balance between two different factors: (i) the hydrogen-bond geometry, influencing the overlap between the SOMO on the NO moiety and the orbitals of the polar substituent (OH, NOH...) on its nearest neighbor; (ii) the relative weight of the polar substituent atoms in the SOMO of the nitroxide. The smaller the hydrogen atom contribution and the larger the electronegative atom (oxygen, nitrogen) contribution to the SOMO, the more likely is a ferromagnetic ordering.

From a methodological point of view, test calculations show that the magnetic coupling (J) has a negligible dependence on the density functional (PBE or BLYP) and the basis set employed in PBC calculations. The inclusion of some Hartree−Fock exchange (as in the PBE0 model) increases spin polarization, possibly modifying the magnetic properties of the nitroxide. However, it cannot change the antiferromagnetic behavior of the compounds under study.

We believe that our results show that PBC-DFT computations give a reliable description of the geometry and of the magnetic properties of nitroxide molecular crystals. They can complement experimental studies in determining the effects influencing the ferromagnetic behavior and in designing new organomagnets. From this point of view, the ability to carry out geometry optimizations seems quite important. Even when the experimental structure of the molecular crystals is available, the position of hydrogen atoms is not always well defined. This

drawback can be nonnegligible when the hydrogen atoms are critical for the transmission of the magnetic coupling as in the present case. Furthermore, the possibility of checking the consequences of chemical modifications on the geometry and on the electronic structure of a given nitroxide is extremely useful in designing new magnetic materials.

Acknowledgment. This work was partially supported by the Italian Reasearch Council (CNR) Grant 99.2282.ST74, by the U.S. National Foundation Grant CHE-9982156, and by Gaussian Inc.

JA011704R